Hindawi
International Journal of Polymer Science
Volume 2021, Article ID 5536047, 9 pages
https://doi.org/10.1155/2021/5536047

Research Article

Stability, Viscosity, and Tribology Properties of Polyol Ester Oil-Based Biolubricant Filled with TEMPO-Oxidized Bacterial Cellulose Nanofiber

Dieter Rahmadiawan[1], **Hairul Abral**[2], **N. Nasruddin**[1] **and Zahrul Fuadi**[3]

[1]*Department of Mechanical Engineering, Universitas Indonesia, Depok 16424, Indonesia*
[2]*Department of Mechanical Engineering, Andalas University, 25163 Padang, Sumatera Barat, Indonesia*
[3]*Department of Mechanical and Industrial Engineering, Universitas Syiah Kuala, Banda Aceh 23111, Indonesia*

Correspondence should be addressed to Hairul Abral; habral@yahoo.com and N. Nasruddin; nasruddin@eng.ui.ac.id

Received 14 January 2021; Revised 18 March 2021; Accepted 2 April 2021; Published 15 April 2021

Academic Editor: Subrata Mondal

This research is aimed at studying the stability and tribology properties of the polyol ester oil- (POE-) based biolubricant mixed with various filler loadings from microparticle of TEMPO-oxidized bacterial cellulose (NDCt) as an additive and sorbitan monostearate (Span 60) as a surfactant. Morphology, rheology, and tribology tests were conducted. The addition of NDCt and Span 60 to pure POE as a base fluid showed elevated viscosity, lower value of coefficient friction (COF), and a remarkable decrease in the wear rate (WR). The presence of 0.6 wt% NDCt and 1.8 wt% Span 60 in POE (N2S4) decreased the COF value by 79% in comparison to POE. At room temperature, this N2S4 biolubricant sample showed a higher thermal conductivity by 4% and lower WR value by 49% compared to POE. This study introduced the preparation of the ecofriendly biolubricant filled with NDCt improving the tribology properties remarkably.

1. Introduction

Development of green lubrication technology with high efficiency, energy saving, and environmentally friendly has attracted great attention recently for many researchers [1]. The demand for using renewable energy in all aspects has led to increased research on natural-based lubricants. [2]. One way to improve lubricant performance is by providing additives. Additives with various functions had been applied and proven to be viscosity improvers, antiwear agents, thermal conductivity enhancer, detergents, etc. [3, 4]. Despite the required technical characteristics, lubricants' pollution and environmental health problems have led to more attention in recent years [5]. A million tons of loss are released into the environment every year [6]. The role of lubricant additives in the world is also vital in environmentally friendly applications [7, 8]. Calcium sulphonates, tricresyl phosphates, and zinc dialkyl dithiophosphates are conventional additives with heavy metals and unhealthy elements [9]. Therefore, the demand for ecofriendly lubricant additives is developing rapidly at present.

Ecofriendly additives from sustainable sources are considered more by researchers rather than conventional additives [8, 10, 11]. A recent study has explored cellulose from the plant as an additive of biolubricant for improvement of its tribology performance [12]. Generally, isolation of the nanocellulose used a chemical treatment. Pure nanocellulose can be obtained from bacterial cellulose (BC) without the need for acid hydrolysis which provides environmental benefits [13]. Source of BC is *Komagataeibacter xylinus*, a bacterium commonly used for the production of *nata de coco* [14]. BC has high thermal and mechanical resistance, a high degree of crystallinity, low cost, and density [15].

BC is hydrophilic in nature and has a large number of hydroxyl groups [16]. The disintegrated hydrophilic BC alone is agglomerated in hydrophobic synthetic lubricant reducing its tribology performance. Individual cellulose nanofiber dispersed in a lubricant is essential. Using 2,2,6,6-

tetramethylpiperidine-1-oxyl (TEMPO) is a usual method to reduce the agglomeration of the cellulose [17]. TEMPO also has the antiwear ability and the free radical group which could enhance the oxidative stability of POE oil [17–19]. Better stability of the individual fibers in lubricant plays an important role in the improvement of the tribology properties of the lubricant [20]. Treatment of cellulose using a surfactant is a common strategy to look for the better stability of the cellulose in a lubricant. Recently, Span 60 has been used as a surfactant improving the stability of the nanofluid [21, 22]. A surfactant also has the antiwear ability, which, once again, in this case, is very suitable as lubricant additives [23].

Numerous works have reported a biolubricant filled with cellulose [24–26]. Recent research which is relatively similar to our present investigation has quantified the characterization of biolubricant mixed with cellulose from plant [12, 27, 28]. However, the study on tribology performance and viscosity of POE-based biolubricant mixed with NDCt as an additive and Span 60 as a surfactant is yet to be explored. Therefore, the present work is aimed at preparing this biolubricant which was filled with various filler loadings of NDCt and Span 60. Stability and tribology performance of the biolubricant were explored and discussed.

2. Materials and Methods

2.1. Materials. 2,2,6,6-Tetramethylpiperidine-1-oxyl (TEMPO) with the purity of 98%, Span 60, sodium hypochlorite (NaClO), and sodium bromide (NaBr) were purchased from Sigma-Aldrich Company. POE (Emkarate) was obtained from The Lubrizol Corporation. Wet BC pellicle (300 mm × 300 mm × 10 mm) as a raw material for TEMPO-oxidized bacterial cellulose (NDCt) was purchased from a small local market in Padang, West Sumatera, Indonesia. The dried BC nanofiber has a crystallinity index of 80% [15].

2.2. Preparation of Disintegrated NDCt. Figure 1 illustrates the working flow of this research. The wet BC was soaked with NaOH (10 wt%) for 24 h to remove the impurity and then washed several times with distilled water until pH 7. This wet pellicle was disintegrated using an electrical blender for 30 minutes. The wet disintegrated BC was dried using a drying oven (Memmert UN-55) at 75°C for three days. The dried BC film (about 5 g) was reblended and manually ground using porcelain mortar to form a small particle powder and then filtered using a handmade sieve (100 mesh) to obtain a homogeneous particle size.

The dried BC particle was treated using a solution mixed with TEMPO at room temperature. The treatment process was similar as reported by a previous study with a little modification [29]. The dried BC powder (5 g) was suspended into a solution from distilled water (300 ml), TEMPO (0.1 g), NaBr (0.3 gr), and NaClO (30 ml). The mixture was stirred using a plate stirrer (Daihan Scientific MSH-200) at 350 rpm for 2 h. The suspension was filtered using a custom sieve (500 mesh) and neutralized with ethanol (250 ml) for several times until pH 7, then fibrillated by a high-speed homogenizer (IKA T-25) at 12000 rpm for 30 min. This NDCt/ethanol suspension was used as an additive in POE.

2.3. Preparation of Biolubricant. Biolubricant from the mixture of NDCt/Span 60/POE was prepared by the following method as shown in Table 1. POE oil as the base fluid was compounded with various NDCt and Span 60 loadings. NDCt and Span 60 with a ratio of 1 : 2 and 1 : 3 were dispersed into the POE oil. Firstly, Span 60 was dissolved in POE oil and stirred using a hot plate stirrer (Daihan Scientific MSH-200) at 75°C for 30 min [26]. Further, the NDCt/ethanol suspension was slowly added and then stirred at 110°C for 2 h to evaporate the remaining ethanol until constant weight and reach the exact amount as the composition of the designed sample in Table 1. The obtained biolubricants were homogenized using high-speed homogenizer (IKA T-25) at 12000 rpm for 15 min to disperse fillers in the suspension.

2.4. Stability via Photo Capturing. The stability of the biolubricant (NDCt/Span 60 in POE) as a function of time was observed using the same method that is used in the literature, photo capturing [28, 30]. A conventional camera was used to capture each sample (20 ml) in a glass bottle at various time intervals for 0, 24, 48, 120, 240, and 720 h.

2.5. Morphology Investigation of BC and Wear Scar of the Disk. Surface morphology of the dried NDCt sample was observed using FE-SEM (JFIB4610, JEOL) with 15 kV and 8 mA. Before the FE-SEM observation, each NDCt sample was coated using a gold evaporator system for 10 s and 10 mA to reduce electron charge. Furthermore, the NDCt size in suspension was measured using a particle size analyzer (PSA) from Shimadzu SALD-2300 instrument equipped with a cyclone injection-type dry measurement unit, "SALD-DS5," a batch cell-sample dispersion unit, "SALD-BC23" (approximately 12 ml). The measurement unit used to investigate the NDCt particle was a semiconductor laser operating at 680 nm. The morphology of the wear scar of the disk was investigated using SEM (FEI QUANTA 650).

2.6. FTIR. The FTIR was determined with Spectrum Two-UATR (Perkin Elmer, United States) which is integrated with a detector of MIR TGS to detect the spectra. The scanning range of the measurements was 500–4000 cm^{-1} with a scanning speed of 0.2 cm/s.

2.7. Thermal Conductivity. Thermal conductivity of PO and biolubricants are measured using a KD2 thermal property analyzer (Decagon, USA, version 5). This equipment works with the principle of a transient hot-wire technique. The KS-1 sensor (60 mm length, 1.27 mm diameter) was used for the thermal conductivity measurement. A circulating thermostatic bath was used for controlling the samples' temperature within ±1°C. Thermal conductivity of PO and biolubricants are investigated within a temperature range of 20 to 60°C. Each sample was measured with five repetitions. Identification of the significance of any differences in thermal conductivity between PO and biolubricants was carried out using one-way analysis of variance (ANOVA) and a p-test.

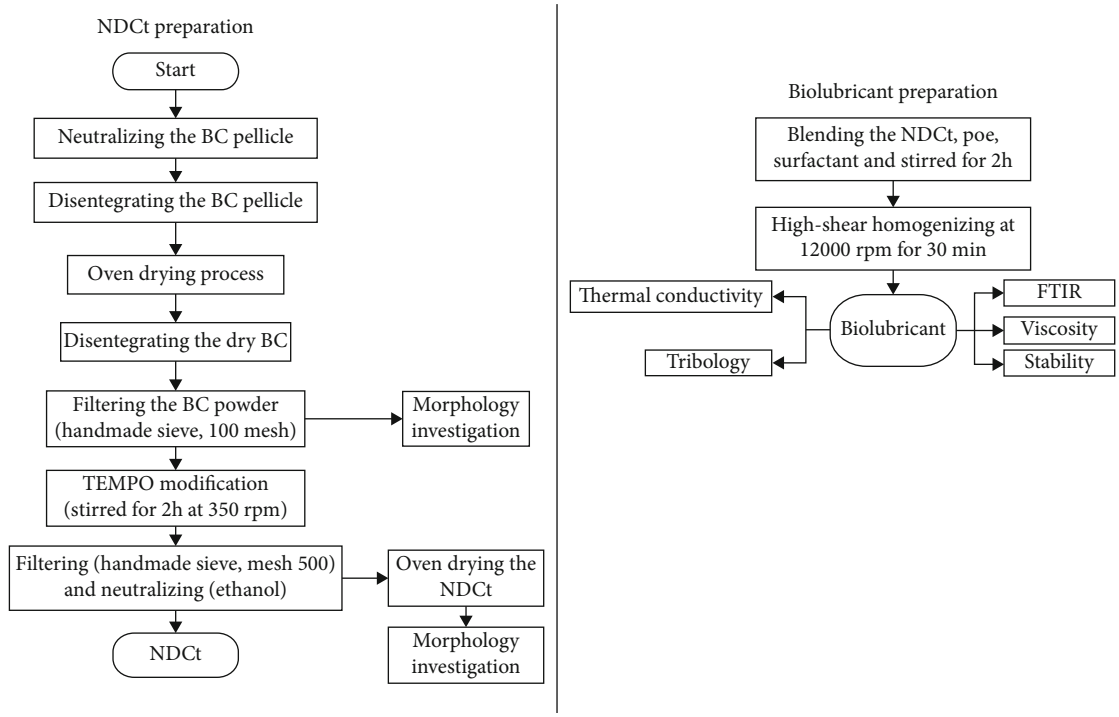

Figure 1: Flowchart of NDCt and biolubricant preparation.

Table 1: The composition of NDCt (N) and Span 60 (S) in the POE biolubricant.

Sample	Ratio of NDCt to Span 60	Mass fraction (wt%)		
		POE	NDCt	Span 60
PO	0	100	0	0
N1S2	1 : 2	99.1	0.3	0.6
N1S3	1 : 3	98.8	0.3	0.9
N2S4	2 : 4	98.2	0.6	1.2

Duncan multiple range tests were subsequently used using a 95% ($p \leq 0.05$) confidence level. Experimental data were analyzed using IBM SPSS Statistics 25.0 (IBM Corporation, Chicago, USA).

2.8. Viscosity. DHR-1 rheometer (TA Instruments, USA) accompanied by a 40 mm diameter parallel geometry was used to measure the viscosity of the samples. The samples were placed between parallel plates with a diameter of 40 mm and a gap of 1000 μm and equilibrated at 20°C for 4 min. The analysis conducted with a defined shear rate at room temperature.

2.9. Tribology. The tribological tests were conducted using a tribometer designed by Fuadi et al. [31]. Briefly, the equipment has an AISI52100 ball (diameter of 8 mm) and a grey cast iron disk (30 mm diameter) with a thickness of 5 mm. The surface roughness of both the ball and the disk was about 0.04 μm. The friction test was carried out with a sliding speed of 200 rpm at room temperature and a normal load of 5.5 N. The initial contact pressure between the ball and disk surfaces was 989 MPa (Hertzian) as simulating friction in boundary lubrication regimes. Wear rate (WR) of the disk and ball with the unit of (mm^3/N m) is calculated using Equation (1) [32]:

$$\mathrm{WR} = \frac{\Delta V}{F \times S}, \tag{1}$$

where ΔV is the volume loss (mm^3), S is the sliding distance of the ball (m), and F is the load applied to the disk (N). Volume loss for the disk is calculated using Equation (2).

$$\Delta V = 2\pi R\left[\mathrm{r}^2 \sin^{-1}\left(\frac{d}{2r}\right) - \left(\frac{d}{4}\right)\left(4r^2 - \mathrm{d}^2\right)^{1/2}\right], \tag{2}$$

where R is the radius of the wear scar, r is the diameter of the ball, and d is the diameter of the wear scar.

3. Results and Discussion

3.1. The Physical Appearance of BC Nanofiber. Figure 2 shows the FE-SEM morphology of (a) the BC film (before TEMPO treatment) and (b) the NDCt film (after the mash and high-shear homogenization process). Both films had many interlinked BC nanofibers from intermolecular hydrogen bonding [14]. The diameter of a BC nanofiber was less than 100 nm (see Figures 2(a) and 2(b)). Figure 2(c) displays the distribution of the NDCt size in suspension. The average value of the NDCt was about 230 μm, smaller than that of the BC powder (250 μm) without TEMPO treatment. The reduction of this size was attributable to the process of mash and homogenizing which may disintegrate some BC fibers as shown in Figure 2(b) (brown arrow).

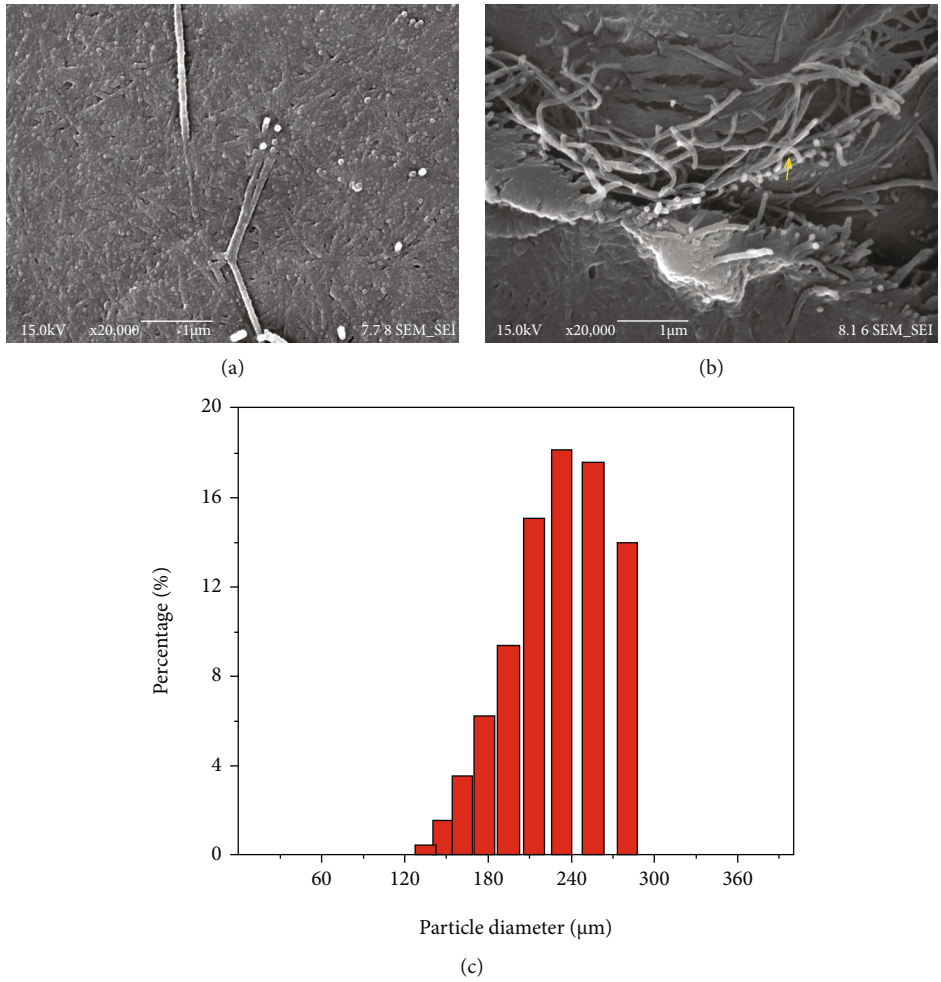

Figure 2: FE-SEM of (a) BC film, (b) the NDCt film, and (c) NDCt size in suspension after measuring using a PSA.

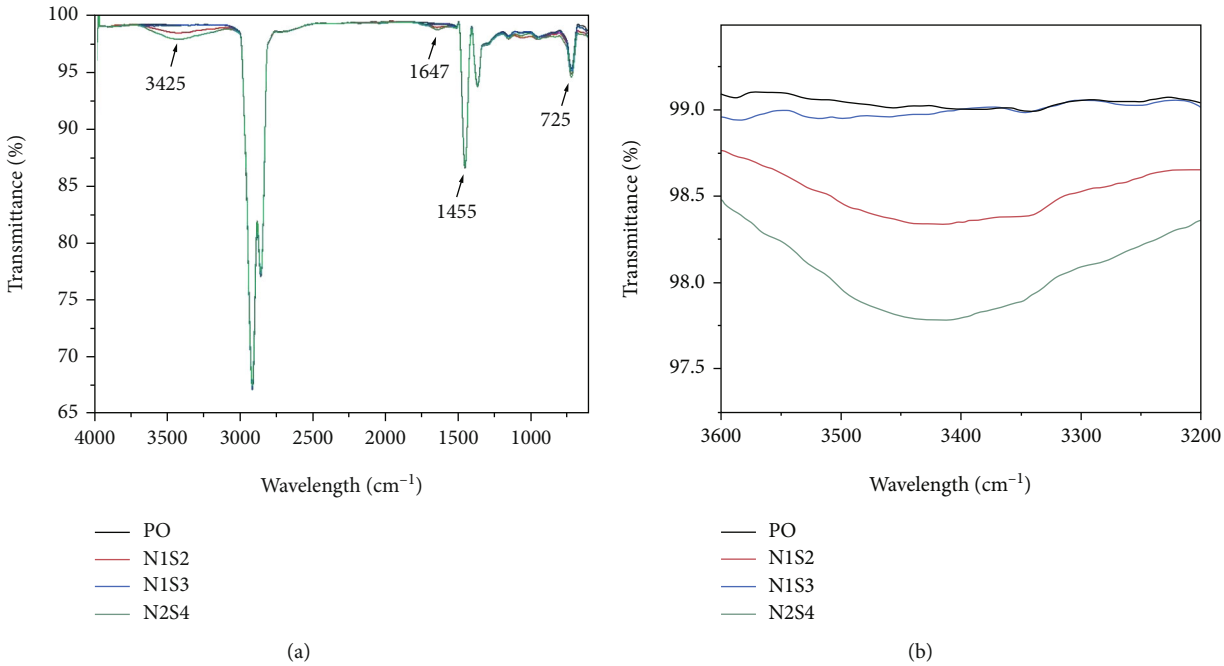

Figure 3: FTIR spectra of PO and biolubricant with (a) complete spectrum and (b) sections of the hydroxyl groups.

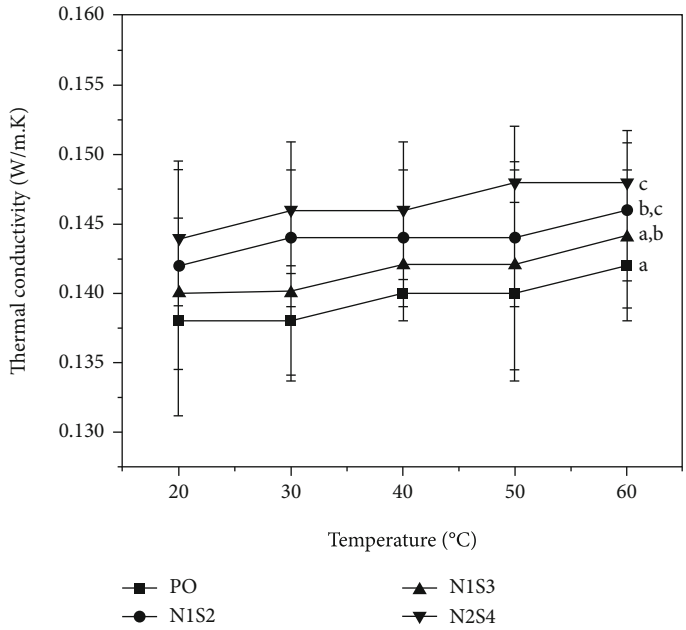

Figure 4: Thermal conductivity of PO and biolubricants. Different subscripts (a, b, c) indicate significant differences at $p \leq 0.05$.

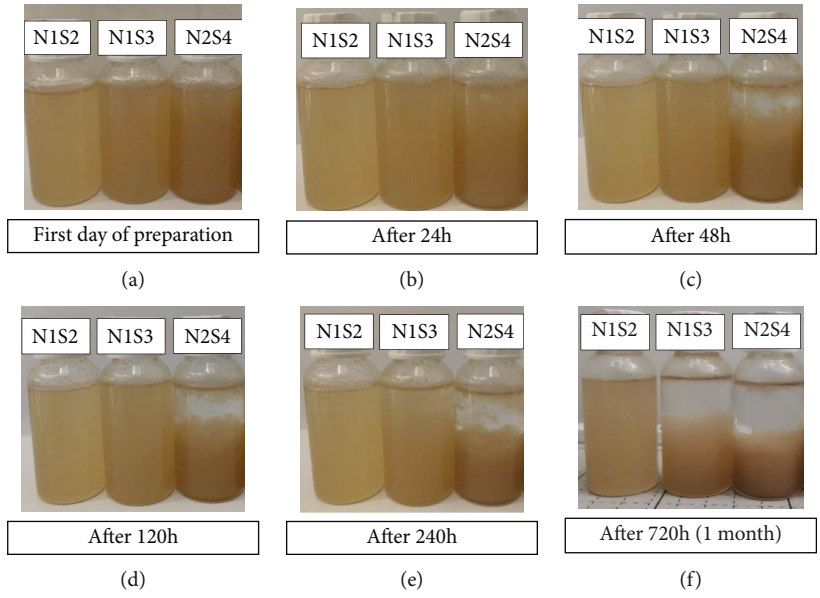

Figure 5: Stability observation of biolubricants at particular time.

3.2. FTIR. The FTIR spectra of biolubricants were shown in Figure 3. All samples display a similar form of the spectrum, but the difference in the bands and intensity. Figure 3(b) presents O-H stretching vibration in the range of 3100-3500 cm^{-1} which is a characteristic of the bacterial cellulose nanofiber [15]. A band of –C=O groups at the peak of 1647 cm^{-1} confirms ester corresponds to the POE's methyl group [33]. The peak at 1455 cm^{-1} belongs to $–CH_2$ groups of alkyl chains [34, 35]. A band at the peak of 725 cm^{-1} is due to the presence of C–H vibrations [33]. PO sample did not have a peak of the O-H functional group (Figure 3(b)). As expected, the addition of NDCt in the PO sample led to the broader band and stronger intensity shown by the N1S2 and N2S4 samples. The strongest intensity was observed on the N2S4 sample corresponding to the highest amount of NDCt in the fluid [36]. However, the N1S3 biolubricant displays weaker intensity of the peak of the O-H group than the N1S2 sample. This is probably a result of an excessive amount of surfactant which is more hydrophobic than NDCt [37].

3.3. Thermal Conductivity. Figure 4 showed the thermal conductivity of the PO and biolubricant samples as a function of temperature. Increasing temperature improved the thermal conductivity resulting from an increase of the Brownian

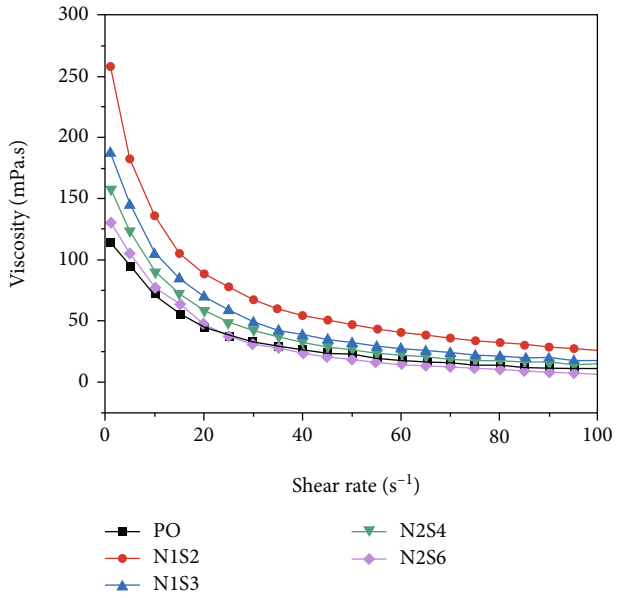

Figure 6: Viscosity of PO and biolubricants.

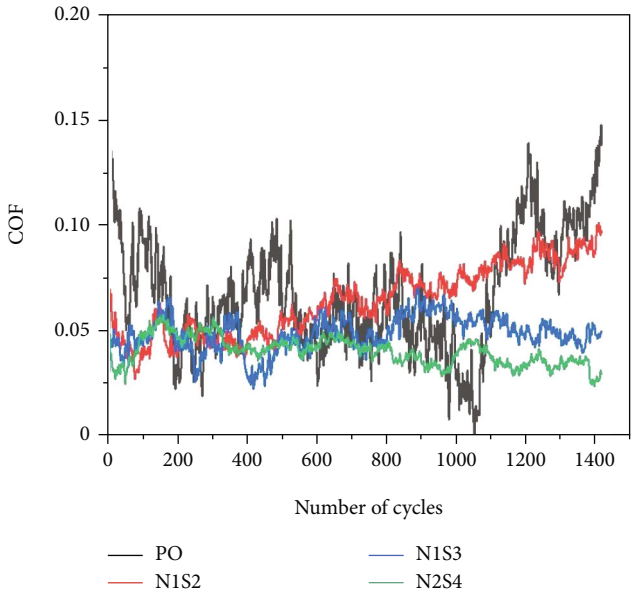

Figure 7: The friction coefficient of PO and biolubricants.

motion of nanoparticles [38]. Biolubricants had higher thermal conductivity compared to the PO sample. This corresponds to the thermal conductivity of bacterial cellulose (0.9 W/m.K) which is higher than POE (0.14 W/m.K) at room temperature [16]. Adding NDCt and Span 60 with ratio 1 : 2 to the PO sample led to a significant increase ($p < 0.05$) in thermal conductivity of the biolubricant. The most conductive sample was measured on the N2S4 biolubricant with the average value of 0.146 W/mK (at 60°C) which is increased significantly by 4% compared to PO sample. This increment is because the mobility of the NDCt particle in the fluid-created microscopic motion which caused microconvection [39]. Further adding the NDCt particle into the fluid will create faster motion due to more intense van der

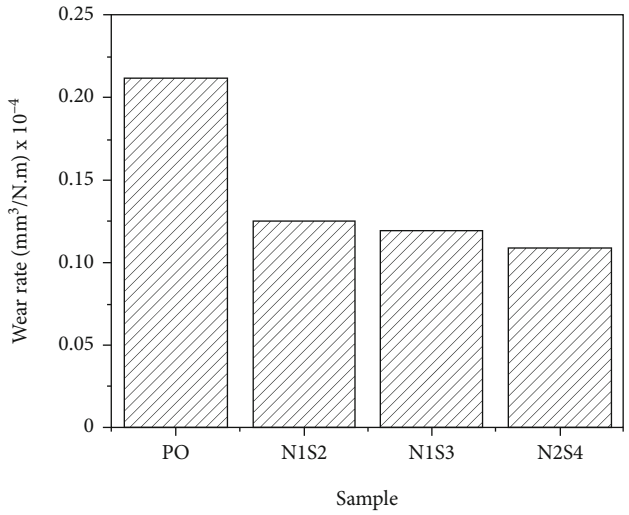

Figure 8: The wear rate for the lubricants under speed of 200 rpm and 5.5 N load.

Wall forces between the NDCt particles, which increases the heat transfer process [39]. Thermal conductivity of the N1S3 sample was lower than the case of N1S2 probably as a result of excessive surfactant which is consistent with Figure 3.

3.4. Stability and Viscosity. To stabilize the fibers in the oil, a low hydrophilic-lipophilic balance (HLB) of surfactant is required [20]. Span 60 has an HLB value of 4.7, which is ideal in this condition [24]. The qualitative sedimentation method via photo capturing was used to observe the biolubricant's stability, as presented in Figure 5. A good stability nanofluid is indicated with no more than 30% sedimentation after a month [40]. It shows that N1S2 is the most stable sample with no NDCt accumulation at the bottom of the test tube after a month of sedimentation observation (Figure 5(f)).

On the other hand, the N2S4 sample was sedimented after two days of investigation (Figure 5(c)). The N1S2 and N2S4 samples have the same NDCt and Span 60 ratios (1 : 2). The N1S2 sample obtained better stability than the N2S4. This result is probably due to the higher concentration of the surfactant (span 60) decreasing the viscosity of biolubricants, thus increasing the particle's sedimentation velocity due to the effect of the faster Brownian motion and higher activity of van der Wall forces [41].

Figure 6 shows the viscosity of all samples measured with increasing shear rate ranges from 5 to 100/s at 25°C. It can be seen that the viscosity of the biolubricant is increased with the addition of NDCt. The N1S2 sample has the highest viscosity compared to POE. A decrease in viscosity occurs when the amount of the surfactant is increased. The N2S4 sample had the lowest viscosity value compared to other biolubricant samples. This tendency corresponds to a high concentration of Span 60 reducing the viscosity value [42]. The long chain of saturated hydrocarbon molecules in POE can crystallize with the alkane groups from Span 60; thus, the POE bonds become weaker [42].

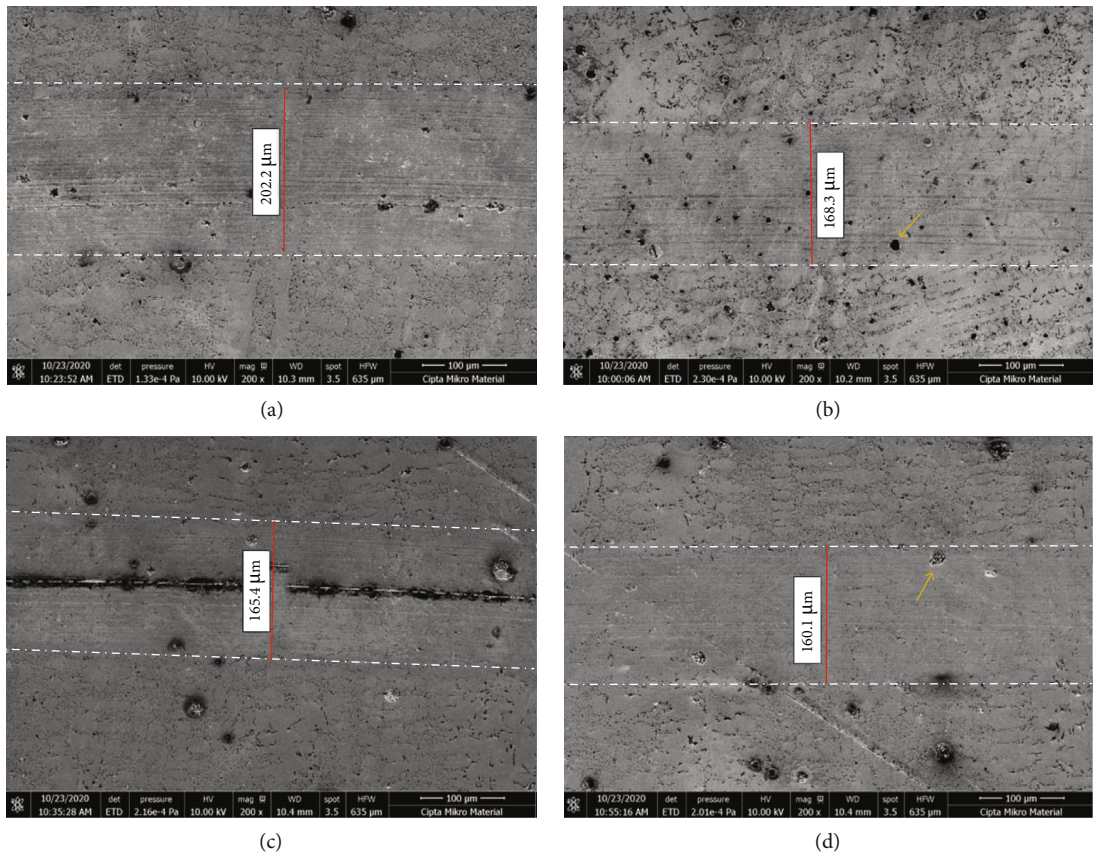

Figure 9: The SEM micrographs of wear scar width (distance between two white dash-dot lines) on the surface of grey cast iron disk after the friction test using (a) PO, (b) N1S2, (c) N1S3, and (d) N2S4. Brown arrows indicate black pits.

3.5. Tribological Studies (Friction and Worn Analysis). The coefficient of friction (COF) along the cycle number for each sample is displayed in Figure 7. The PO without filler shows the rougher curve during the running-in period probably because of higher friction between the ball and disk surface [12]. After the addition of fillers (NDCt and Span 60) in POE, the curve became smoother due to lower friction. At the cycle number of 1395, the N2S4 sample displayed the lowest COF value (0.024), a decrease of 79% compared with POE (0.1). This is consistent with Figure 8 showing the addition of NDCt and Span 60 into POE decreased the WR of sliding surfaces. The lowest WR value was observed on the N2S4 sample, reduced to 49% compared to the PO sample. This tendency is also supported by Figure 9 showing the SEM surface morphology of worn block on the disk surface after using each sample. As shown in the figure, the wear scar width (the distance between two white dash-dot lines) after using the biolubricant was reduced. The width value of the PO, N1S2, N1S3, and N2S4 samples directly measured from SEM observation was 202.2, 168.3, 165.4, and 160.1 μm, respectively. The lowest value for the N2S4 sample corresponds to the smallest contact between the sliding surface resulting from the formation of a triboboundary film from the biolubricant between these sliding surfaces [43]. The use of this N2S4 sample also resulted in the smoothest surfaces and the fewest number of black pits (brown arrow in Figure 9(d)) on the wear track area. This phenomenon may be the nanosized NDCt fibers which fill the scars and grooves of the rubbing surface (the mending and polishing effect) minimize surface roughness [44]. These results are similar to a previous research on lubrication performance of polyalphaolefin oil with cellulose nanocrystals [27]. This work observed a COF improvement of 30% compared to the base oil.

4. Conclusion

This research work has explored tribology properties of the biolubricant prepared from POE mixed with the NDCt microparticle and Span 60. The results have demonstrated that the NDCt effectively improved the tribological properties of the base oil. The addition of NDCt as an additive in POE has decreased the wear rate and the wear scar as a result of the decreased contact between the sliding surfaces. The best tribology performance was found on the N2S4 sample from mixing of 0.6 wt.% of NDCt and 1.2 wt% surfactant. The use of this sample reduced the average COF value of about 40% and resulted in the smallest contact between the sliding surface, the smoothest surfaces of the wear tracks, and the maximum wear rate reduction of about 49% compared with POE. These results offer deeper insights into the effect of fillers on the improvement of tribology properties of ecofriendly biolubricant prepared from bacterial cellulose nanofibers.

Data Availability

The participants of this study agree for their data to be shared publicly.

Conflicts of Interest

We affirm that there is no conflict of interest.

Acknowledgments

This study was supported by the Hibah Publikasi di Jurnal Internasional terindeks Scopus, tahun 2021; the Jurusan Teknik Mesin, Fakultas Teknik, Universitas Andalas, tahun 2021; and the Research and Development Directorates Universitas Indonesia for supporting research funding with project name "PUTI KI 2Q2," number NKB-787UN2.RST/HKP.05.00/2020.

References

[1] M. Z. Sharif, W. H. Azmi, A. A. M. Redhwan, R. Mamat, and G. Najafi, "Energy saving in automotive air conditioning system performance using SiO 2/PAG nanolubricants," *Journal of Thermal Analysis and Calorimetry*, vol. 135, no. 2, pp. 1285–1297, 2019.

[2] W. K. Shafi, A. Raina, and M. I. Ul Haq, "Performance evaluation of hazelnut oil with copper nanoparticles - a new entrant for sustainable lubrication," *Industrial Lubrication and Tribology*, vol. 71, no. 6, pp. 749–757, 2019.

[3] I. Minami, "Molecular science of lubricant additives," *Applied Sciences*, vol. 7, no. 5, p. 445, 2017.

[4] R. Anand, A. Raina, M. I. Ul Haq, M. J. Mir, O. Gulzar, and M. Wani, "Synergism of TiO2and graphene as nano-additives in bio-based cutting fluid-an experimental investigation," *Tribology Transactions*, pp. 1–18, 2021.

[5] H. Wu, F. Jia, J. Zhao et al., "Effect of water-based nanolubricant containing nano-TiO_2 on friction and wear behaviour of chrome steel at ambient and elevated temperatures," *Wear*, vol. 426-427, pp. 792–804, 2019.

[6] S. Gryglewicz and B. Kolwzan, "Synthesis and biodegradation of synthetic oils based on adipic and sebacic esters," *Journal of Synthetic Lubrication*, vol. 20, no. 4, pp. 281–288, 2004.

[7] A. Z. Syahir, N. W. M. Zulkifli, H. H. Masjuki et al., "A review on bio-based lubricants and their applications," *Journal of Cleaner Production*, vol. 168, pp. 997–1016, 2017.

[8] S. Shankar, M. Manikandan, D. K. Karupannasamy, C. Jagadeesh, A. Pramanik, and A. K. Basak, "Investigations on the tribological behaviour, toxicity, and biodegradability of kapok oil bio-lubricant blended with (SAE20W40) mineral oil," *Biomass Conversion and Biorefinery*, pp. 1–13, 2021.

[9] R. K. Hewstone, "Environmental health aspects of lubricant additives," *Science of the total environment*, vol. 156, no. 3, pp. 243–254, 1994.

[10] R. Kumar, M. I. Ul Haq, A. Raina, and A. Anand, "Industrial applications of natural fibre-reinforced polymer composites – challenges and opportunities," *International Journal of Sustainable Engineering*, vol. 12, no. 3, pp. 212–220, 2019.

[11] I. Bhushan, V. K. Singh, and D. K. Tripathi, *Nanomaterial and Enviromental Biotechnology*, Springer, Cham, 2020.

[12] N. W. Awang, D. Ramasamy, K. Kadirgama, G. Najafi, and N. A. Che Sidik, "Study on friction and wear of cellulose nanocrystal (CNC) nanoparticle as lubricating additive in engine oil," *International Journal of Heat and Mass Transfer*, vol. 131, pp. 1196–1204, 2019.

[13] N. Din, N. R. Gilkes, B. Tekant, R. C. Miller, R. A. J. Warren, and D. G. Kilburn, "Non-hydrolytic disruption of cellulose fibres by the binding domain of a bacterial cellulase," *Bio/Technology*, vol. 9, no. 11, pp. 1096–1099, 1991.

[14] D. Klemm, E. D. Cranston, D. Fischer et al., "Nanocellulose as a natural source for groundbreaking applications in materials science: today's state," *Materials Today*, vol. 21, no. 7, pp. 720–748, 2018.

[15] H. Abral, V. Lawrensius, D. Handayani, and E. Sugiarti, "Preparation of nano-sized particles from bacterial cellulose using ultrasonication and their characterization," *Carbohydrate Polymers*, vol. 191, pp. 161–167, 2018.

[16] K. Uetani, T. Okada, and H. T. Oyama, "In-plane anisotropic thermally conductive nanopapers by drawing bacterial cellulose hydrogels," *ACS Macro Letters*, vol. 6, no. 4, pp. 345–349, 2017.

[17] Z. Tang, W. Li, X. Lin et al., "TEMPO-oxidized cellulose with high degree of oxidation," *Polymers*, vol. 9, no. 12, p. 421, 2017.

[18] D. Li, P. Gao, X. Sun, S. Zhang, F. Zhou, and W. Liu, "The study of TEMPOs as additives in different lubrication oils for steel/steel contacts," *Tribology International*, vol. 73, pp. 83–87, 2014.

[19] T. Saito, S. Kimura, Y. Nishiyama, and A. Isogai, "Cellulose nanofibers prepared by TEMPO-mediated oxidation of native cellulose," *Biomacromolecules*, vol. 8, no. 8, pp. 2485–2491, 2007.

[20] W. Yu and H. Xie, "A review on nanofluids: preparation, stability mechanisms, and applications," *Journal of Nanomaterials*, vol. 2012, 17 pages, 2012.

[21] M. A. Khairul, K. Shah, E. Doroodchi, R. Azizian, and B. Moghtaderi, "Effects of surfactant on stability and thermophysical properties of metal oxide nanofluids," *International Journal of Heat and Mass Transfer*, vol. 98, pp. 778–787, 2016.

[22] H. W. Xian, N. A. C. Sidik, and R. Saidur, "Impact of different surfactants and ultrasonication time on the stability and thermophysical properties of hybrid nanofluids," *International Communications in Heat and Mass Transfer*, vol. 110, p. 104389, 2020.

[23] S. A. Savrik, D. Balköse, and S. Lku, "Synthesis of zinc borate by inverse emulsion technique for lubrication," *Journal of Thermal Analysis and Calorimetry*, vol. 104, no. 2, pp. 605–612, 2011.

[24] K. Gao, Q. Chang, and B. Wang, "The dispersion and tribological performances of magnesium silicate hydroxide nanoparticles enhanced by Span 60 oleogel," *Journal of Sol-Gel Science and Technology*, vol. 94, no. 1, pp. 165–173, 2020.

[25] L. Yu, M. Dong, B. Ding, and Y. Yuan, "Emulsification of heavy crude oil in brine and its plugging performance in porous media," *Chemical Engineering Science*, vol. 178, pp. 335–347, 2018.

[26] K. Uvanesh, S. S. Sagiri, K. Senthilguru et al., "Effect of span 60 on the microstructure, crystallization kinetics, and mechanical properties of stearic acid oleogels : an in-depth analysis," *Journal of Food Science*, vol. 81, no. 2, pp. E380–E387, 2016.

[27] K. Li, X. Zhang, C. Du et al., "Friction reduction and viscosity modification of cellulose nanocrystals as biolubricant additives

in polyalphaolefin oil," *Carbohydrate Polymers*, vol. 220, pp. 228–235, 2019.

[28] N. W. Awang, D. Ramasamy, K. Kadirgama, M. Samykano, G. Najafi, and N. A. Che Sidik, "An experimental study on characterization and properties of nano lubricant containing cellulose nanocrystal (CNC)," *International Journal of Heat and Mass Transfer*, vol. 130, pp. 1163–1169, 2019.

[29] C. Huang, H. Ji, Y. Yang et al., "TEMPO-oxidized bacterial cellulose nanofiber membranes as high-performance separators for lithium-ion batteries," *Carbohydrate polymers*, vol. 230, p. 115570, 2020.

[30] I. M. Shahrul, I. M. Mahbubul, R. Saidur, and M. F. M. Sabri, "Experimental investigation on Al_2O_3-W, SiO_2-W and ZnO-W nanofluids and their application in a shell and tube heat exchanger," *International Journal of Heat and Mass Transfer*, vol. 97, pp. 547–558, 2016.

[31] Z. Fuadi, K. Adachi, and T. Muhammad, "Formation of carbon-based tribofilm under palm methyl ester," *Tribology Letters*, vol. 66, no. 3, p. 88, 2018.

[32] M. Fellah, M. Abdul Samad, M. Labaiz, O. Assala, and A. Iost, "Sliding friction and wear performance of the nano-bioceramic α-Al_2O_3 prepared by high energy milling," *Tribology International*, vol. 91, pp. 151–159, 2015.

[33] V. Bonu, N. Kumar, A. Das, S. Dash, and A. K. Tyagi, "Enhanced lubricity of SnO2 nanoparticles dispersed polyolester nanofluid," *Industrial and Engineering Chemistry Research*, vol. 55, no. 10, pp. 2696–2703, 2016.

[34] T. Aging and A. Munajad, "Fourier transform infrared (FTIR) spectroscopy analysis of transformer paper in mineral oil-paper composite insulation under accelerated thermal aging," *Energies*, vol. 11, no. 2, p. 364, 2018.

[35] F. Niu, M. Li, Q. Huang et al., "The characteristic and dispersion stability of nanocellulose produced by mixed acid hydrolysis and ultrasonic assistance," *Carbohydrate Polymers*, vol. 165, pp. 197–204, 2017.

[36] Y. Chen, F. Wang, L. Dong et al., "Design and optimization of flexible polypyrrole/bacterial cellulose conductive nanocomposites using response surface methodology," *Polymers*, vol. 11, no. 6, p. 960, 2019.

[37] D. H. Khan, S. Bashir, P. Figueiredo, H. A. Santos, M. I. Khan, and L. Peltonen, "Process optimization of ecological probe sonication technique for production of rifampicin loaded niosomes," *Journal of Drug Delivery Science and Technology*, vol. 50, pp. 27–33, 2019.

[38] M. R. Esfahani, E. M. Languri, and M. R. Nunna, "Effect of particle size and viscosity on thermal conductivity enhancement of graphene oxide nanofluid," *International Communications in Heat and Mass Transfer*, vol. 76, pp. 308–315, 2016.

[39] K. H. Solangi, S. N. Kazi, M. R. Luhur et al., "A comprehensive review of thermo-physical properties and convective heat transfer to nanofluids," *Energy*, vol. 89, pp. 1065–1086, 2015.

[40] L. Samylingam, K. Anamalai, K. Kadirgama et al., "Thermal analysis of cellulose nanocrystal-ethylene glycol nanofluid coolant," *International Journal of Heat and Mass Transfer*, vol. 127, pp. 173–181, 2018.

[41] A. Ghadimi, R. Saidur, and H. S. C. Metselaar, "A review of nanofluid stability properties and characterization in stationary conditions," *International Journal of Heat and Mass Transfer*, vol. 54, no. 17-18, pp. 4051–4068, 2011.

[42] X. Gu, L. Gao, Y. Li et al., "Performance and mechanism of span surfactants as clean flow improvers for crude oil," *Petroleum Chemistry*, vol. 60, no. 1, pp. 140–145, 2020.

[43] L. Kerni, A. Raina, and M. I. U. Haq, "Friction and wear performance of olive oil containing nanoparticles in boundary and mixed lubrication regimes," *Wear*, vol. 426-427, pp. 819–827, 2019.

[44] G. Liu, X. Li, B. Qin, D. Xing, Y. Guo, and R. Fan, "Investigation of the mending effect and mechanism of copper nanoparticles on a tribologically stressed surface," *Tribology Letters*, vol. 17, no. 4, pp. 961–966, 2004.